EARTHQUAKE ENGINEERING AND STRUCTURAL DYNAMICS
Earthquake Engng. Struct. Dyn. **27**, 397–412 (1998)

A MODAL PROCEDURE FOR SEISMIC ANALYSIS OF NON-LINEAR BASE-ISOLATED MULTISTOREY STRUCTURES

PASQUALE MALANGONE[1]*† AND MASSIMILIANO FERRAIOLI[2]‡

[1] *Dipartimento di Ingegneria Civile, Seconda Università di Napoli, via Roma 29, Aversa, Caserta 81031, Italia*
[2] *Dipartimento di Ingegneria Civile, Università di Salerno, Ponte don Melillo, Fisciano, Salerno 84084, Italia*

SUMMARY

A modal procedure for non-linear analysis of multistorey structures with high-damping base-isolation systems was proposed. Two different isolation devices were considered in the analysis: an high-damping laminated rubber bearing and a lead-rubber bearing. Starting from deformational properties verified by tests, the isolation systems were characterized using three different analytical models (an Elastic Viscous, a Bilinear Hysteretic and a Wen's Model) with parameters depending from maximum lateral strain. After non-linear modelling of isolation and lateral-force-resisting systems, the effects of material non-linearities were considered as pseudo-forces applied to the equivalent linear system (Pseudo-Force Method) and the formally linearized equations of motion were uncoupled by the transformation defined by the complex mode shapes. The modal responses were finally obtained with an extension of Nigam–Jennings technique to non-linear and non-classically damped systems, in conjunction with an iterative technique searching for non-linear contributions satisfying equations of motion and constitutive laws. Since the properties of the isolated structure usually change with maximun lateral strain of isolation bearings, the integration of a new set of governing equations was required for each design-displacement value.

The procedure proposed was described in detail and then applied for the determination of modal and total seismic responses in some real cases. At first, a very good agreement between non-linear responses obtained with the proposed mode superposition and with a direct integration method was observed. Then a comparison of results obtained with the three different analytical models of the isolation bearings was carried out. At last, the exact modal response obtained with analytical models depending from the design displacement of the isolation bearings was compared with two different approximated solutions, evaluated using mode shapes and isolation properties, respectively, calculated under simplified hypothesis. © 1998 John Wiley & Sons, Ltd.

KEY WORDS: isolation bearings; base-isolated structures; non-linear modelling; modal superposition

INTRODUCTION

It is well known that aseismic base isolation of structures is an important design strategy for protecting buildings from earthquake strong ground motions. In the recent years, several studies have been carried out in order to understand the performance of base-isolation devices and systems. Extensive reviews on recent developments on the subject were provided by Kelly[1,2]. Fan *et al.*[3,4] described seismic responses of several base-isolation systems, including rubber bearings with and without lead core, the sliding joint, the french system, resilient-friction isolators with and without upper sliding plate. Skinner *et al.*[5] studied the deformational characteristics of a great number of isolation bearings, such as steel hysteretic dampers, lead-extrusion

* Correspondence to: Pasquale Malangone, Dipartimento di Ingegneria Civile, Seconda Università degli Studi di Napoli, via Roma 29, Aversa, Caserta 81031, Italia
† Professor
‡ Graduate Research Assistant

CCC 0098–8847/98/040397–16$17·50
© 1998 John Wiley & Sons, Ltd.
Received 12 December 1995
Revised 6 February 1997 and 14 August 1997

dampers and lead-rubber bearings. On the other side, an inelastic model of the lateral-force-resisting system was often considered for the evaluation of structural damage and seismic safety under earthquake strong ground motions.

According to UBC[6] criteria selection of the lateral response procedure, the static analysis may be used for the design of seismic-isolated structures only for particular seismic zones, site characteristics, structural configurations and isolation properties. As a consequence, dynamic lateral-response procedure (with response spectrum or time-history analysis) and inelastic modelling (including the deformational characteristics of isolation system and structural elements above the isolation interface) are often required.

The non-linear dynamic response is usually obtained by direct integration methods of the equations of motion.[7] This conventional approach requires the solution of a system of differential equations whose size is equal to the total number of degrees of freedom of the isolated structure. Moreover, since seismic response may be strongly dependent from maximum displacement of isolation bearings, the solution of a new system of equations for each design-displacement attempt value is usually required. On the other side, the complex mode superposition can give several advantages not only for the evaluation but also for the understanding of seismic response of isolated structures. Moreover, it has been found to be competitive in terms of computational effort with direct integration methods in numbers of simple non-linear dynamic problems.[8–11]

In this study, a mathematical model including the force–deflection characteristics of non-linear elements of isolation and lateral-force-resisting systems was adopted. As far as the two isolation bearings considered, three different analytical models with parameters depending from the maximum lateral displacement (an Elastic Viscous, a Bilinear Hysteretic and a Wen's Model) were characterized starting from prototype tests. For the structural elements above the isolation interface an elastoplastic model was considered in the analysis. The dynamic response was obtained taking non-linearities as pseudo-forces on the right-hand side of the equations of motion, and using a complex mode superposition and an iterative technique for the associated linear system subjected to effective inertia forces. The modal procedure was applied for the analysis of isolated structures with different fixed-base fundamental periods. For the isolation systems and the analytical models considered, the agreements between exact modal response and approximated solutions obtained with mode shapes and isolation properties independent from the maximum displacement of the bearings were finally investigated.

ANALYTICAL MODEL OF ISOLATION BEARINGS

An high-damping laminated rubber bearing (HDLRB) and a lead-rubber bearing (LR) were considered in the analysis. The force–deflection properties were obtained with sequences of horizontal displacements cycles performed at different vertical loads and rates of loading[12,5] (Figures 1 and 2). Tests results show that the dynamic properties in horizontal shear depend on maximum displacement D and, particularly, the effective stiffness K_{sp} of isolation bearings is proportional to displacement raised to the α_K power, while the energy dissipation W is proportional to displacement raised to the α_W power (with $\alpha_K = -0{\cdot}373$ and $\alpha_W = 1{\cdot}57$ for the HDLRB; $\alpha_K = -0{\cdot}582$ and $\alpha_W = 1{\cdot}53$ for the LR system). Finally, it is to be observed that the behaviour of the two bearings considered is not consistent with a linear elastic and linear viscous model, for which W is quadratic and K_{sp} is independent from displacement (that is $\alpha_W = 2$ and $\alpha_K = 0$).

Elastic-viscous model with parameters depending on maximum displacement

Using this model, the reactive force $F_0(x_0, \dot{x}_0)$ of the isolation bearing is expressed in the form

$$F_0(x_0, \dot{x}_0) = K_{sp}(D) \cdot x_0(t) + C(D) \cdot \dot{x}_0(t) \tag{1}$$

© 1998 John Wiley & Sons, Ltd.

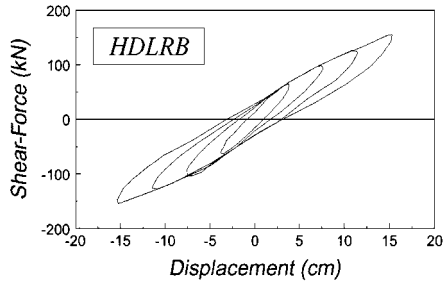

Figure 1. HDLRB isolation system: force-displacement loops verified by tests

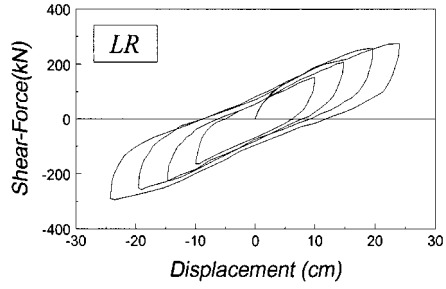

Figure 2. LR isolation system: force-displacement loops verified by tests

where $K_{sp}(D)$ is the effective stiffness at the design displacement D, while the coefficient $C(D)$ of viscous damping is evaluated from the effective damping $\beta(D)$ given by

$$\beta = \frac{W(D)}{2 \cdot \pi \cdot K_{sp}(D) \cdot D^2} \tag{2}$$

The elastic-viscous model here proposed gives a good approximation to the variations verified by tests of effective stiffness K_{sp} and energy dissipation W with maximum displacement D of the isolation bearing. However, this linearly viscous model is not consistent with experimental results which show the independence of energy dissipation from loading rate.

Bilinear-hysteretic model with parameters depending on maximum displacement

This model with only hysteretic damping gives the reactive force of the isolation bearing as a function of design and yield displacements D and $D_y(D)$, and of elastic and post-yield stiffnesses $K_{b1}(D)$ and $K_{b2}(D)$. These analytical parameters were characterized assuming that the co-ordinates of the points of maximum and minimum displacements, the energy dissipation and the post-yield stiffness have the same values verified by tests and using the method of least squares to fit experimental results (Figures 3 and 4; Table I). It is to be observed that the bilinear-hysteretic model here proposed is consistent with the variation of effective stiffness and energy dissipation with maximum displacement and loading rate. On the contrary, a bilinear model with constant isolation parameters gives energy dissipation as a linear function of displacement (that is $\alpha_W = 1$) and effective stiffness proportional to displacement raised to the $\alpha_K = -1$ power.

Wen's model with parameters depending on maximum displacement

The hysteretic restoring force of the isolation bearings is approximated by the expression

$$F_0(x_0, \dot{x}_0) = \alpha(D) \cdot \frac{F_y(D)}{d_y(D)} \cdot x_0(t) + [1 - \alpha(D)] \cdot F_y(D) \cdot z(t) \tag{3}$$

© 1998 John Wiley & Sons, Ltd.

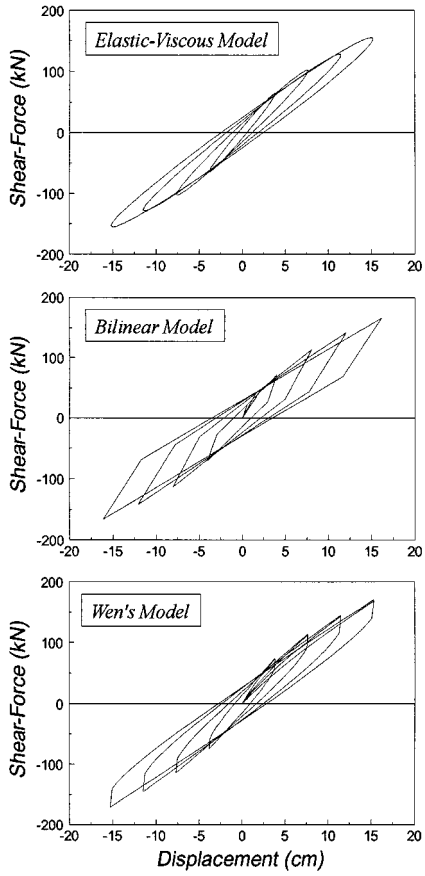

Figure 3. HDLRB isolation system: analytical approximation to force–displacement loops

where the dimensionless hysteretic displacement $z(t)$ satisfies the following differential equation:

$$\dot{z}(t)\cdot d_y = -\gamma\cdot|\dot{x}_0(t)|\cdot z(t)\cdot|z(t)|^{\eta-1} - \beta\cdot\dot{x}_0(t)\cdot|z(t)|^{\eta} + \theta\cdot\dot{x}_0(t) \tag{4}$$

In equations (3) and (4), $F_y(D)$ and $d_y(D)$ are the yielding force and displacement; $\alpha(D)$ is the post- to pre-yielding stiffness ratio; η is a parameter governing the transition from elastic to plastic response; θ and $\gamma/\beta = \psi$ control the loading and unloading phases; $[\theta/(\gamma+\beta)]^{1/\eta}$ influences the maximum value of the restoring force. The values of isolation parameters were calculated assuming the same maximum displacement, effective stiffness and energy dissipation verified by tests and fitting the experimental results (Figures 3 and 4; Table I). As a consequence, the proposed Wen's model with variable parameters gives a good approximation to the plots of effective stiffness and energy dissipation with maximum displacement and loading rate.

STRUCTURAL MODEL AND GOVERNING EQUATIONS

The modal procedure is introduced with reference to a multistorey shear-type structure mounted on base-isolation bearings (Figure 5). An elastoplastic model incorporating the force–deflection characteristics of non-linear elements is considered for the structure. The isolation system is characterized using

© 1998 John Wiley & Sons, Ltd.

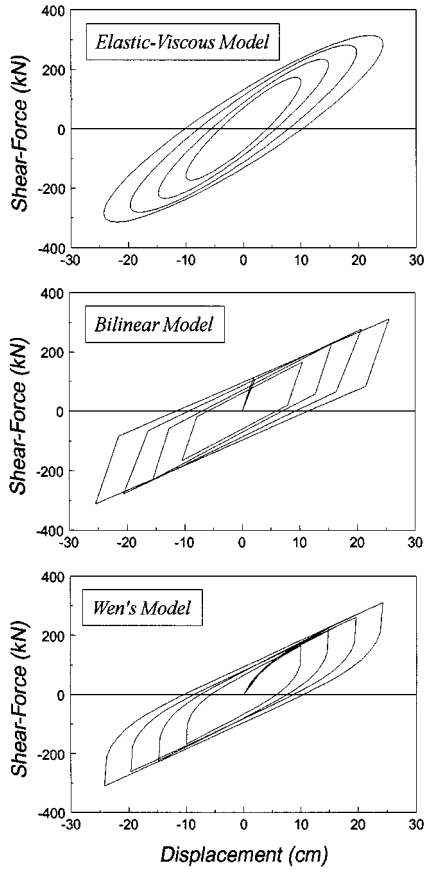

Figure 4. LR isolation system: analytical approximation to force–displacement loops

Table I. HDLRB and LR isolation bearings: parameters of analytical models

Elastic-viscous model				Bilinear-hysteretic model			Wen's model					
D (cm)	K_{sp} (kN/cm)	C (kN·s/cm)	β (per cent)	D_y (cm)	K_{b1} (kN/cm)	K_{b2} (kN/cm)	d_y (cm)	F_y (kN)	α	η	θ	ψ
High damping laminated rubber bearing (HDLRB system)												
3·82	16·10	0·647	10·9	0·917	27·51	12·72	0·455	23·56	0·271	0·15	2·0	− 1·5
7·64	12·72	0·571	10·8	1·025	29·49	10·85	0·875	31·21	0·312	0·15	2·0	− 1·5
11·47	10·79	0·564	11·6	1·571	25·91	9·263	1·295	43·06	0·303	0·15	2·0	− 1·5
15·18	9·572	0·504	11·0	1·233	30·14	8·262	1·715	41·93	0·369	0·15	2·0	− 1·5
Lead-rubber bearing (LR system)												
10·0	15·80	2·267	18·0	1·295	56·25	10·11	0·030	68·11	0·00440	0·05	0·25	0·5
14·8	14·67	1·909	16·7	1·408	60·37	10·12	0·035	80·35	0·00428	0·05	0·25	0·5
19·7	13·14	1·818	15·5	2·164	48·93	9·249	0·036	82·47	0·00403	0·05	0·25	0·5
24·3	11·75	1·730	15·7	2·010	56·46	8·431	0·042	95·77	0·00392	0·05	0·25	0·5

© 1998 John Wiley & Sons, Ltd.

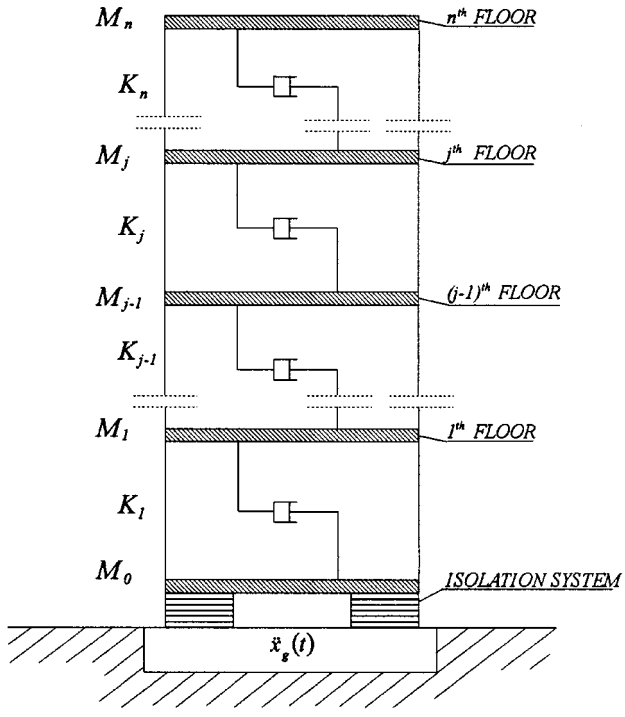

Figure 5. Structural model of a n-storey base-isolated building

deformational properties verified by tests and considering the three different analytical models just described. The base-shear may be expressed as the sum of linear and non-linear contributions in the following form:

$$F_0(t) = K_b(D) \cdot x_0(t) + F_{NL}(t) \tag{5}$$

where the linear stiffness $K_b(D)$ and the non-linear term $F_{NL,0}(t)$ depend on the force–displacement characteristics of the analytical model considered for the isolation bearings. Particularly, $K_b(D) = K_{sp}(D)$ and $F_{NL,0}(t) = 0$ for the elastic-viscous model; $K_b(D) = \alpha(D) \cdot F_y(D)/d_y(D)$ and $F_{NL,0}(t) = [1 - \alpha(D)] \cdot F_y(D) \cdot z(t)$ for the Wen's model. For the bilinear-hysteretic model $K_b(D) = K_{b1}(D)$, while the non-linear contribution in elastic phase is constant and in yielding phase is given by

$$F_{NL,0}(t) = [K_{b2}(D) - K_{b1}(D)] \cdot [x_0(t) - D_y(D)\,\mathrm{sgn}(\dot{x}_0(t))] \tag{6}$$

In the same way, the jth floor shear (with $j = 1 \ldots n$, where n is the number of degrees of freedom of the structure) may be expressed as the sum of a linear contribution $K_j \cdot \Delta x_j(t)$ and a non-linear contribution $F_{NL,j}(t)$ in the following form:

$$F_j(t) = K_j \cdot \Delta x_j(t) + F_{NL,j}(t) \tag{7}$$

Using equations (5) and (7) leads to the total reactive force vector $\{R_t(t)\}$ expressed in the following matrix form:

$$\{R_t(t)\} = [K_t(D)]\{x_t(t)\} + \{R_{t\,NL}(t)\} \tag{8}$$

© 1998 John Wiley & Sons, Ltd.

where is

$$\{R_t(t)\} = \begin{Bmatrix} R_0(t) \\ \{R(t)\} \end{Bmatrix}, \quad \{x_t(t)\} = \begin{Bmatrix} x_0(t) \\ \{x(t)\} \end{Bmatrix}, \quad \{R_{t\,NL}(t)\} = \begin{Bmatrix} R_{NL,0}(t) \\ \{R_{NL}(t)\} \end{Bmatrix} \tag{9}$$

while $[K_t(D)]$ is the total stiffness matrix of the isolated structure and the vector $\{R_{t\,NL}(t)\}$ is obtained from the non-linear contributions to the floor shears. From equation (8) the equations of motion of non-linear base-isolated multistorey structures subjected to earthquake ground motion may be written in the form

$$[M_t]\cdot\{\ddot{x}_t(t)\} + [C_t]\cdot\{\dot{x}_t(t)\} + [K_t(D)]\cdot\{x_t(t)\} = -[M_t]\cdot\{I_t\}\cdot\ddot{x}_g(t) - \{R_{t\,NL}(t)\} \tag{10}$$

where $\{\ddot{x}_t(t)\}$, $\{\dot{x}_t(t)\}$ and $\{x_t(t)\}$ are the acceleration, velocity and displacement relative to the ground vectors, $\ddot{x}_g(t)$ is the ground acceleration, $\{I_t\}$ is an influence vector.

The mass, damping and stiffness matrices $[M_t]$, $[C_t(D)]$, $[K_t(D)]$ of the isolated structure are defined by substructuring as follows:

$$[M_t] = \begin{bmatrix} M_b & \{0\}^T \\ \{0\} & [M] \end{bmatrix}, \quad [C_t] = \begin{bmatrix} C_b(D) + C_0 & \{C_{sp}\}^T \\ \{C_{sp}\} & [C] \end{bmatrix}, \quad [K_t(D)] = \begin{bmatrix} K_b(D) + K_0 & \{K_{sp}\}^T \\ \{K_{sp}\} & [K] \end{bmatrix} \tag{11}$$

In equation (11), M_b, $C_b(D)$ and $K_b(D)$ are, respectively, the base mass, the coefficient of viscous damping and the linear stiffness of the isolation system (primary system); C_0 and K_0 account for the increase of base damping and stiffness deriving from the presence of the structure (secondary system); $[M]$, $[C]$ and $[K]$ are, respectively, the mass, damping and elastic stiffness matrices of the structure; $\{C_{sp}\}$ and $\{K_{sp}\}$ are the coupling vectors between structure and base mass (secondary system/primary system). Particularly, the damping matrix $[C]$ of the fixed-base structure is characterized in the hypothesis of *Clough damping*, while the coefficients C_0 and K_0 and the vectors $\{C_{sp}\}^T$ and $\{K_{sp}\}^T$ are given by

$$C_0 = \sum_{j,k=1}^{n} C_{j,k}\,, \qquad K_0 = K_1 \tag{12}$$

$$\{C_{sp}\}^T = \left\{ -\sum_{j=1}^{n} C_{j,1}\,; \ldots ; -\sum_{j=1}^{n} C_{j,k}; \ldots ; -\sum_{j=1}^{n} [C]_{j,n} \right\}, \quad \{K_{sp}\}^T = \{-K_1 \;\; 0 \;\; \cdots \;\; 0\} \tag{13}$$

INTEGRATION OF GOVERNING EQUATIONS

Because of the strong differences between the internal mechanism of energy dissipation, the base isolated structures are usually non-classically damped: as an alternative to direct integration methods, equation (10) may be uncoupled only in the complex field. Particularly, using the complex mode superposition leads to the following expression of the displacement vector (Appendix I):

$$\{x_t(t)\} = 2\,Re\left(\sum_{j=1}^{n+1} \{\underline{\Phi}_j(D)\}\cdot Z_j(t) \right) \tag{14}$$

In equation (14), $\{\underline{\Phi}_j(D)\}$ is the lower-half of the jth complex mode shape, and $Z_j(t)$ is the modal co-ordinate obtained from the uncoupled equation:

$$\dot{Z}_j(t) - p_j(D)\cdot Z_j(t) = G_j(D)\cdot g_j(t) \tag{15}$$

where $p_j(D) = -\xi_j(D)\cdot\omega_j + i\cdot\omega_{dj}(D)$ is the jth complex eigenvalue, $G_j(D)$, is the participation factor and $g_j(t)$ is the modal pseudo-acceleration. The modal solution $Z_j(t)$ is here obtained with a step-by-step integration method which extends the well-known *Nigam–Jennings* procedure to modal equations of base-isolated systems. This method leads to the following iterative formula:

$$\begin{Bmatrix} Re(Z_j(t)) \\ Im(Z_j(t)) \end{Bmatrix} = [\tilde{A}(D)] \begin{Bmatrix} Re(Z_j(t-\Delta t)) \\ Im(Z_j(t-\Delta t)) \end{Bmatrix} + [\tilde{B}(D)] \begin{Bmatrix} \ddot{x}_g(t-\Delta t) + u_j(t-\Delta t) \\ \ddot{x}_g(t) + u_j(t) \end{Bmatrix} + [\tilde{C}(D)] \begin{Bmatrix} v_j(t-\Delta t) \\ v_j(t) \end{Bmatrix} \tag{16}$$

© 1998 John Wiley & Sons, Ltd.

where $[\tilde{A}(p_j(D), \Delta t)]$, $[\tilde{B}(p_j(D), \Delta t)]$ and $[\tilde{C}(p_j(D), \Delta t)]$ are system characteristic matrices depending from the fixed time integration-step Δt and from the jth complex eigenvalue $p_j(D)$ (Appendix II). The terms $u_j(t)$ e $v_j(t)$ have to be calculated at each integration step by an iterative technique, searching for the non-linear contributions satisfying both equations of motion and constitutive laws.[13]

It is to be noted that the non-linear response of isolated structures is generally dependent on the maximum lateral displacement of the isolation bearings. As a consequence, an iterative procedure to obtain the calculated peak-displacement $D_c = \max|x_0(t)|$ and the initial design-displacement value D coincident with the fixed tolerance is needed. This means that the solution of a new non-linear dynamic problem and the calculation of complex mode shapes and system characteristic matrices $[\tilde{A}]$, $[\tilde{B}]$ and $[\tilde{C}]$ are usually required at each iteration. However, approximations to the *Exact Modal Solution* can be obtained using isolation parameters defined for a fixed value of design displacement. Particularly, an approximated value of the design displacement of the isolation bearing is given by the peak-displacement D_{BF} obtained under the hypothesis of very stiff fixed-base structure ($T_{BF} \cong 0$), that is with the non-linear analysis of an equivalent single degree of freedom system.

In this work two different approximated solutions are considered. The first (*Fixed Mode-Shapes Solution*) is obtained using an isolation model depending on maximum lateral strain (that is $[\tilde{A}] = [\tilde{A}(D)]$, $[\tilde{B}] = [\tilde{B}(D)]$ and $[\tilde{C}] = [\tilde{C}(D)]$) and considering the superposition of fixed mode shapes calculated at the approximated design-displacement value D_{BF} (that is $\{\Phi_j\} = \{\Phi_j(D_{BF})\}$). The second (*Fixed Design-Displacement Solution*) is evaluated with an analytical model independent from maximum lateral strain and characterizing the isolation properties at the displacement D_{BF} (that is $[\tilde{A}] = [\tilde{A}(D_{BF})]$, $[\tilde{B}] = [\tilde{B}(D_{BF})]$, $[\tilde{C}] = [\tilde{C}(D_{BF})]$ and $\{\Phi_j\} = \{\Phi_j(D_{BF})\}$).

Finally, it is to be observed that using the approximated solutions gives some advantages for the evaluation of structural response of base-isolated structures. In fact, the *Fixed Mode-Shapes* procedure avoids the solution of the tangent eigenproblem at each design-displacement attempt value; while with the *Fixed Design-Displacement* procedure the calculation of mode shapes and characteristic matrices $[\tilde{A}]$, $[\tilde{B}]$ and $[\tilde{C}]$ of the isolated structure is made one time only.

SOME NUMERICAL RESULTS

The proposed procedure was applied for the non-linear analysis of a five-storey building mounted on high-damping rubber bearings with and without lead core. The superstructure was modelled as an elasto-plastic shear-type plane frame, in the hypothesis of *Clough damping* modelling and linear over the height first mode shape. It was characterized starting from: fixed-base fundamental period T_{BF} (with $0 < T_{BF} < 1$); floor weights W_i (where $W_0 = W_1 = \cdots = W_5 = M \cdot g$, with $M = 0{\cdot}40\ \mathrm{kN\,s^2/cm}$ for the HDLRB and $M = 0{\cdot}883\ \mathrm{kN\,s^2/cm}$ for the LR system); and modal damping ratios ξ_i (with $\xi_1 = 3$ per cent, $\xi_2 = 4$ per cent, $\xi_3 = 5$ per cent, $\xi_4 = 6$ per cent, $\xi_5 = 7$ per cent). The fixed-base structure was designed to withstand a shear force $V_s = 0{\cdot}10 \cdot W_{BF}$, where W_{BF} is the total weight of the superstructure. The total force V_s was then distributed over the height of the structure above the isolation interface according to the formula

$$V_{sj} = \frac{W_j \cdot h_j}{\sum_{i=1}^{5} W_i \cdot h_i} \cdot V_s \tag{17}$$

For the two isolation bearings considered in the analysis, starting from force–displacement properties verified by tests, three different analytical models depending on maximum strain were characterized. The isolated structure period T_{ISO} defined by the following expression:

$$T_{ISO}(D) = 2\pi \sqrt{\frac{\sum_{i=0}^{5} W_i}{g \cdot \sum_{j=1}^{N_{ISO}} K_{sp,j}(D)}} \tag{18}$$

is given by $1{\cdot}40 < T_{ISO} < 1{\cdot}83$ s for the HDLRB, and $2{\cdot}10 < T_{ISO} < 2{\cdot}44$ s for the LR system, depending on maximum lateral displacement of the isolation bearings. An accelerogram generated[14] from the *Eurocode* 8[15]

© 1998 John Wiley & Sons, Ltd.

elastic spectra (with peak ground acceleration $0{\cdot}35 \cdot g$ and length 25 s, for soil class A and structural damping $\xi = 5$ per cent) was used to evaluate the seismic response of base-isolated structures.

Direct integration and complex-mode superposition methods

At first, with reference to the simple ideal case with bilinear isolation devices and *Rayleigh-damping* for the whole isolated structure ($[C_t] = \alpha \cdot [M_t] + \beta \cdot [K_t]$ with $\alpha = 0{\cdot}0290\ s^{-1}$ and $\beta = 5{\cdot}797 \times 10^{-6}$ s calculated from the damping ratios $\xi_1 = 3$ per cent and $\xi_5 = 7$ per cent), a comparison of the results obtained with complex-mode superposition method and *Drain-2-D* program[16] was carried out (Figure 6). It is observed a very good agreement between the non-linear responses calculated with the proposed modal approach and with the direct integration.

Moreover, for the analysed real model with LR isolation bearings the exact non-classical damping and the approximated proportional damping solutions were found to be very different (Figure 7). As a consequence, in this case and adequate non-classical damping modelling is required.

Exact modal and approximated solutions

The exact modal response, obtained with an analytical model depending from the design displacement of the isolation bearings, was then compared with the two different approximated solutions here proposed.

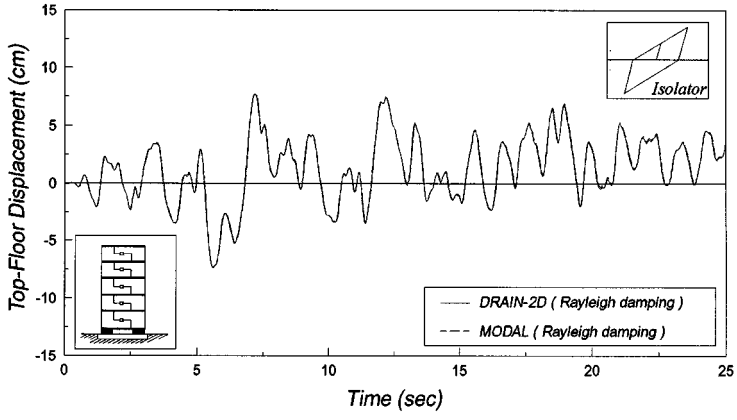

Figure 6. Comparison of top-floor displacement time histories between the proposed procedure and the Drain-2-D program

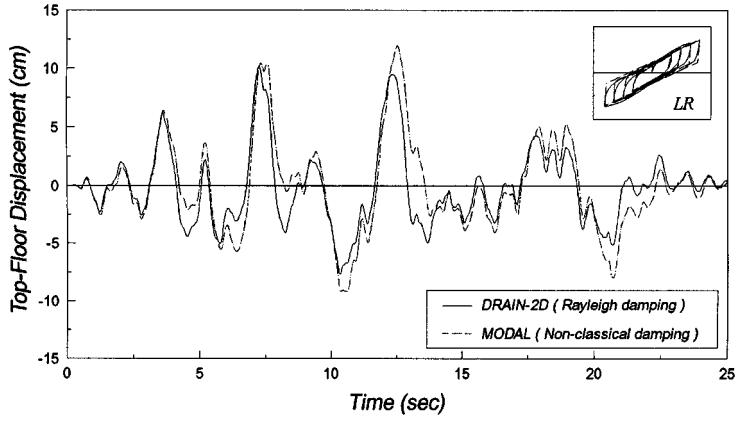

Figure 7. Comparison of top-floor displacement time histories obtained with non-classical and *Rayleigh damping* modelling

© 1998 John Wiley & Sons, Ltd.

After the evaluation of the displacement D_{BF} with the dynamic analysis of the equivalent single degree of freedom system, the *Fixed Mode-Shapes Solution* was obtained considering the superposition of fixed mode shapes calculated at the approximated design-displacement value D_{BF}, while the *Fixed Design-Displacement Solution* was evaluated considering constant isolation properties characterized at the displacement D_{BF}.

The results obtained have shown a good agreement between exact and approximated responses for LR bearings characterized with bilinear and Wen's models. On the contrary, for the elastic-viscous model the *Fixed Mode-Shapes Solution* may be very different: in the absence of isolation non-linear corrections, the superposition of the mode shapes $\{\Phi_j(D_{BF})\}$ gives less accurate solutions (Figure 8). On the other side, for

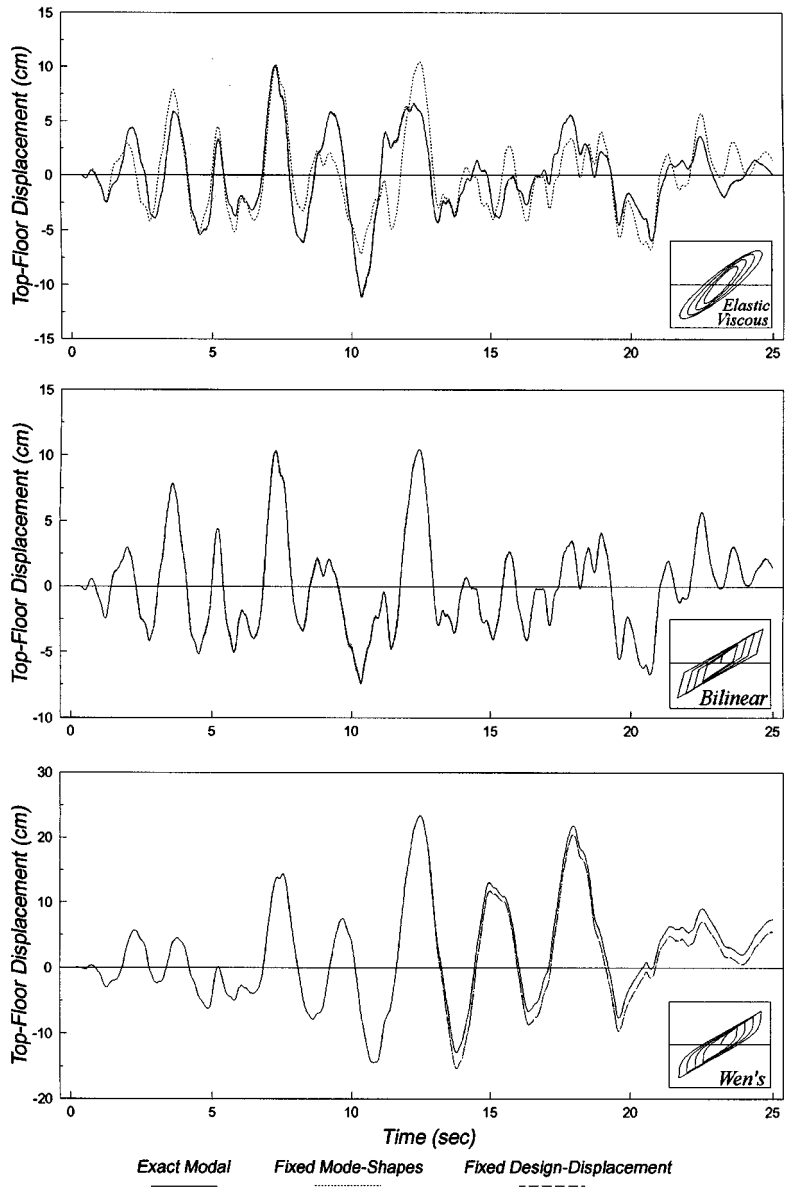

Figure 8. Top-floor displacement time histories: comparison between *Exact Modal Solution* and *Fixed Mode-Shapes* and *Fixed Design-Displacement* approximations ($T_{BF} = 0{\cdot}50$ s, LR isolation system)

© 1998 John Wiley & Sons, Ltd.

the HDLRB system deeper variations between exact and approximated responses, both using viscous and hysteretic models, were found (Figure 9).

Finally, to evaluate the accuracy of modal approximated solutions at fixed-base period T_{BF} variations, a comparison of top-floor acceleration spectra obtained with *Exact Modal*, *Fixed Mode Shapes* and *Fixed Design-Displacement* procedures was carried out. As clearly evident, a very good accuracy of the

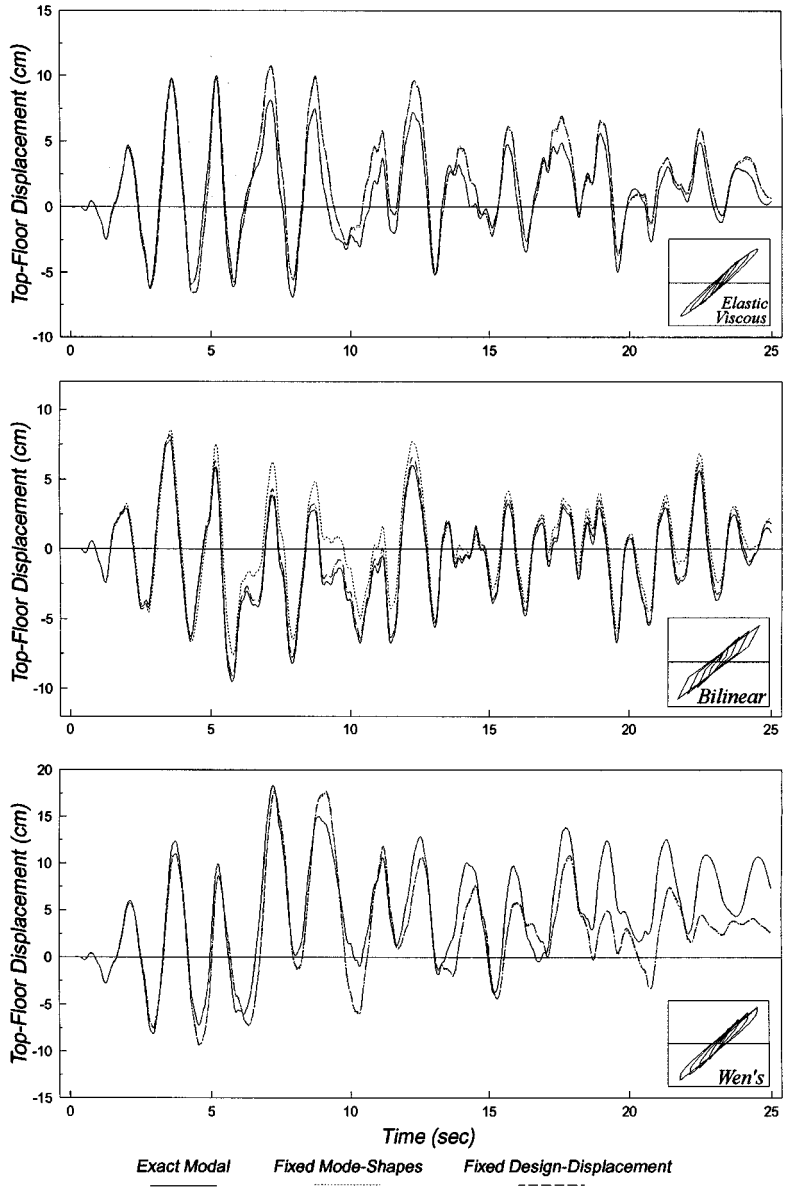

Figure 9. Top-floor displacement time histories: comparison between *Exact Modal Solution* and *Fixed Mode-Shapes* and *Fixed Design-Displacement* approximations ($T_{BF} = 0{\cdot}50$ s, HDLRB isolation system)

© 1998 John Wiley & Sons, Ltd.

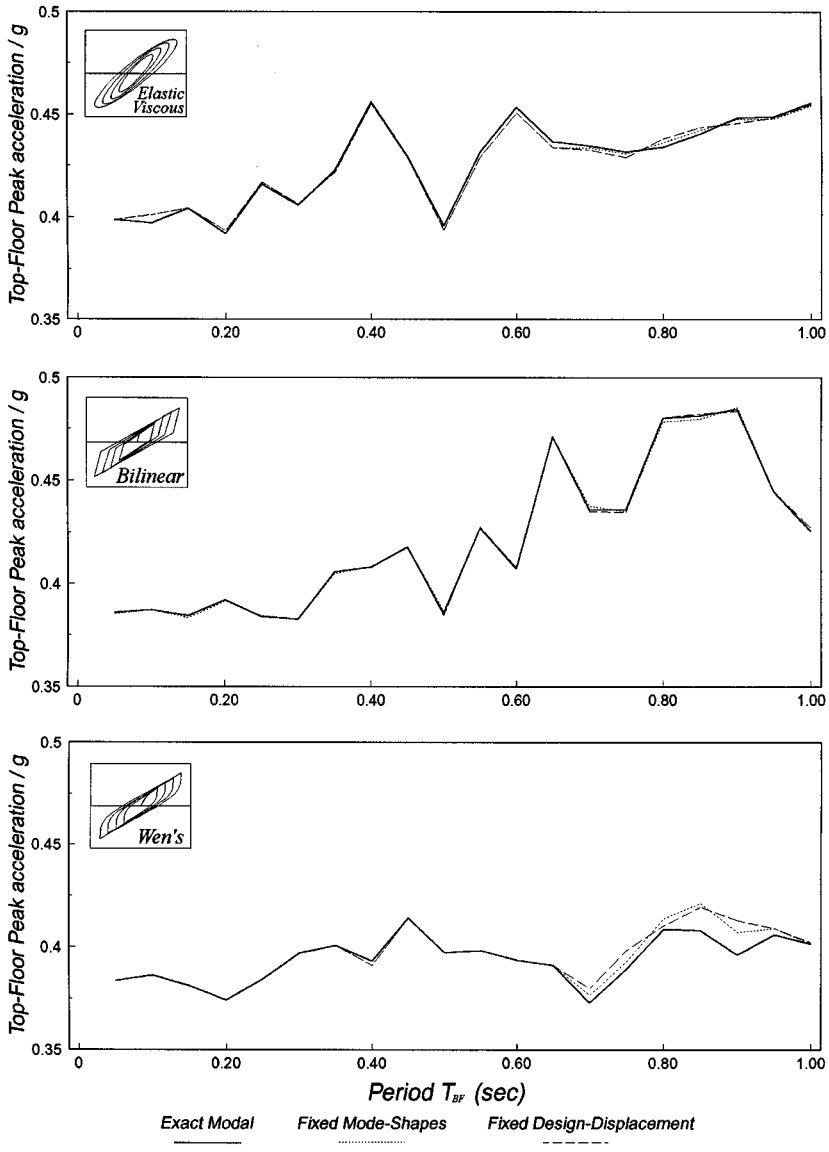

Figure 10. Top-floor acceleration spectra: comparison between *Exact Modal Solution* and *Fixed Mode-Shapes* and *Fixed Design-Displacement* approximations (LR isolation system)

approximated solutions was found for the LR system considered (Figure 10). On the contrary, stronger differences (especially between exact modal and fixed mode-shapes spectra) were noticed for the HDLRB system, both using the elastic viscous and the hysteretic models (Figure 11). These different behaviours derive from the presence of a lead core, which makes LR isolation properties weakly dependent from maximum displacement and produces an increase of hysteretic damping. In other words, for such system the dependence of seismic response from isolation design displacement and fixed-base structure period T_{BF} is greatly reduced (and so $D \cong D(T_{\mathrm{BF}} = 0) = D_{\mathrm{BF}}$).

© 1998 John Wiley & Sons, Ltd.

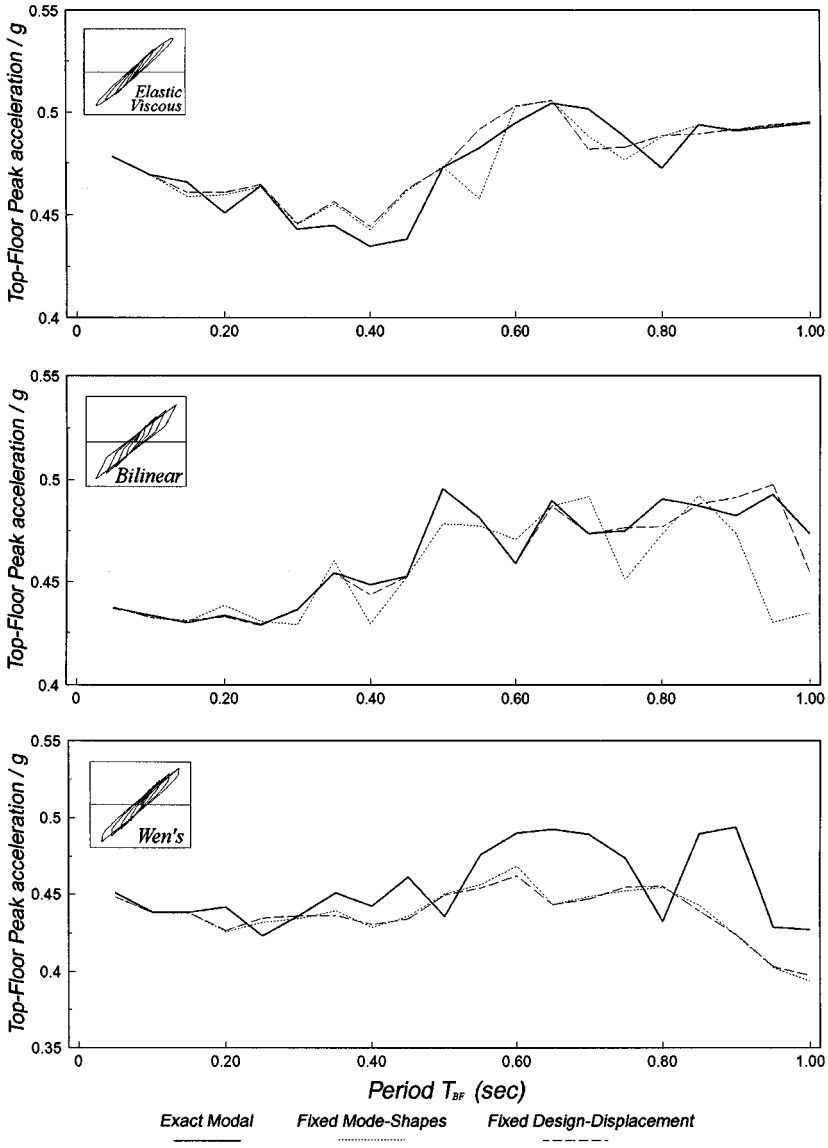

Figure 11. Top-floor acceleration spectra: comparison between *Exact Modal Solution* and *Fixed Mode-Shapes* and *Fixed Design-Displacement* approximations (HDLRB isolation system)

CONCLUSIONS

A modal procedure for non-linear analysis of base isolated multistorey structures was developed. Three different analytical models depending from design displacement of the isolation bearings (Elastic Viscous, Bilinear Hysteretic and Wen's models) were characterized starting from force–displacement dynamic properties verified by tests. After *PFM* linearization and equations uncoupling in the complex field, the modal co-ordinates were computed by a step-by-step integration method in conjunction with a specific iteration technique. The structural response was then obtained using the complex-mode superposition and

© 1998 John Wiley & Sons, Ltd.

an iterative procedure to evaluate the design displacement of the isolation system. As an alternative to this *Exact Modal* procedure, starting from the peak-displacement D_{BF} calculated with non-linear analysis of an equivalent single degree of freedom system, two different approximated procedures were proposed. Particularly, the *Fixed Mode-Shapes Solution* was obtained with an isolation model depending on maximum lateral strain and the superposition of the mode shapes at the displacement value D_{BF}; while the *Fixed Design-Displacement Solution* was evaluated with analytical models with constant parameters characterized at the displacement D_{BF}.

The modal procedure proposed was used for non-linear dynamic analysis of isolated plane frames. The results obtained showed a very good agreement between the non-linear responses calculated with the proposed modal approach and with the direct integration. Moreover, it was observed that for structures with high-damping isolation bearings an adequate non-classical damping modelling may be required. Finally, good agreements between *Exact Modal*, *Fixed Mode Shapes* and *Fixed Design-Displacement Solutions* were found, even for middle–high fixed-base periods, in structures isolated with LR bearings. On the contrary, some differences were observed for the HDLRB system, especially using the Wen's model which is more sensitive to maximum displacements variations. The reason of this different behaviour is the presence of the lead core in the LR system, which reduces the dependence of isolation properties and seismic response from design displacement and fixed-base structure period.

APPENDIX I

Uncoupling of governing equations

The equations of motion are uncoupled in the complex field starting from the following first-order equivalent system:[17–19]

$$[A(D)]\cdot\{\dot{Y}(t)\} + [B(D)]\cdot\{Y(t)\} = \{Q(t)\} \tag{19}$$

where $\{Y(t)\}$ and $\{Q(t)\}$ are, respectively, the state variable and the load vectors given by

$$\{Y(t)\} = \begin{Bmatrix}\{\dot{x}_t(t)\}\\ \{x_t(t)\}\end{Bmatrix}, \qquad \{Q(t)\} = \begin{Bmatrix}\{0\}\\ -[M_t]\cdot\{I_t\}\cdot\ddot{x}_g(t) - \{R_{t\,NL}(t)\}\end{Bmatrix} \tag{20}$$

while $[A(D)]$ e $[B(D)]$ are the following symmetric and positive-definite matrices:

$$[A(D)] = \begin{bmatrix}[0] & [M_t]\\ [M_t] & [C_t(D)]\end{bmatrix}, \qquad [B(D)] = \begin{bmatrix}-[M_t] & [0]\\ [0] & [K_t(D)]\end{bmatrix} \tag{21}$$

Expressing the state variable vector $\{Y(t)\}$ as the sum of the complex mode shapes in the following form:

$$\{Y(t)\} = [\Phi(D)]\cdot\{Z(t)\} \tag{22}$$

and premultiplying by $[\Phi(D)]^T$ the equivalent system (19) becomes

$$[a(D)]\cdot\{\dot{Z}(t)\} + [b(D)]\cdot\{Z(t)\} = -\{l(D)\}\cdot\ddot{x}_g(t) - \{r_{NL}(t)\} \tag{23}$$

where $[a(D)]$ and $[b(D)]$ are diagonal matrices given by

$$[a(D)] = [\Phi(D)]^T\cdot[A(D)]\cdot[\Phi(D)], \quad [b(D)] = [\Phi(D)]^T\cdot[B(D)]\cdot[\Phi(D)] \tag{24}$$

while $\{l(D)\}$ and $\{r_{NL}(t)\}$ are the generalized mass and the non-linear contribution vectors expressed as

$$\{l(D)\} = [\underline{\Phi}(D)]^T\cdot[M_t]\cdot\{I_t\} \tag{25}$$

$$\{r_{NL}(t)\} = [\underline{\Phi}(D)]^T\cdot\{R_{t\,NL}(t)\} \tag{26}$$

in which $[\underline{\Phi}(D)]$ is the lower-half of the elastic mode-shape matrix $[\Phi(D)]$.

© 1998 John Wiley & Sons, Ltd.

The co-ordinate trasformation expressed by equation (22) convert the $2 \cdot N$ (with $N = n + 1$) coupled equation (19) to the following set of uncoupled modal equations:

$$\begin{aligned} &\dot{Z}_j(t) - p_j(D) \cdot Z_j(t) = G_j(D) \cdot g_j(t) \\ &\dot{Z}_j^*(t) - \bar{p}_j(D) \cdot Z_j^*(t) = \bar{G}_j(D) \cdot \bar{g}_j(t) \end{aligned} \quad (j = 1 \ldots N) \tag{27}$$

where $Z_j(t)$ and $Z_j^*(t)$ are, respectively, the jth and $(N + j)$th modal coordinates, $G_j(D)$ and $\bar{G}_j(D)$ are participation factors given by

$$G_j(D) = -\frac{l_j(D)}{a_j(D)}, \quad \bar{G}_j(D) = -\frac{\bar{l}_j(D)}{\bar{a}_j(D)} \tag{28}$$

while $g_j(t)$ and $\bar{g}_j(t)$ are the following modal pseudo-accelerations:

$$g_j(t) = \ddot{x}_g(t) + \frac{1}{l_j} r_{NL,j}(t) \tag{29}$$

$$\bar{g}_j(t) = \ddot{x}_g(t) + \frac{1}{\bar{l}_j} \bar{r}_{NL,j}(t) \tag{30}$$

The $2 \cdot N$ modal coordinates are complex conjugate pairs. Thus, from equation (22) the state variable vector $\{Y(t)\}$ and the displacement vector $\{x_t(t)\}$ can be written in the form

$$\{Y(t)\} = 2\,Re\left(\sum_{j=1}^{N} \{\Phi_j(D)\} \cdot Z_j(t) \right) \tag{31}$$

$$\{x_t(t)\} = 2\,Re\left(\sum_{j=1}^{N} \{\underline{\Phi}_j(D)\} \cdot Z_j(t) \right) \tag{32}$$

APPENDIX II

Terms of system characteristic matrices

$$a_{11} = e^{-\xi_j \omega_j \Delta t} \cos(\omega_{dj} \Delta t) \tag{33}$$

$$a_{12} = -e^{-\xi_j \omega_j \Delta t} \sin(\omega_{dj} \Delta t)$$

$$a_{21} = -a_{12}, \quad a_{22} = a_{11}$$

$$b_{11} = e^{-\xi_j \omega_j \Delta t}[(m_j - r_j/\Delta t)\cos(\omega_{dj}\Delta t) - (n_j - s_j/\Delta t)\sin(\omega_{dj}\Delta t)] + r_j/\Delta t \tag{34}$$

$$b_{12} = e^{-\xi_j \omega_j \Delta t}[r_j \cos(\omega_{dj}\Delta t) - s_j \sin(\omega_{dj}\Delta t)]/\Delta t - (m_j + r_j/\Delta t)$$

$$b_{21} = e^{-\xi_j \omega_j \Delta t}[(m_j - r_j/\Delta t)\sin(\omega_{dj}\Delta t) + (n_j - s_j/\Delta t)\cos(\omega_{dj}\Delta t)] + s_j/\Delta t$$

$$b_{22} = e^{-\xi_j \omega_j \Delta t}[(r_j \sin(\omega_{dj}\Delta t) + s_j \cos(\omega_{dj}\Delta t)]/\Delta t - (n_j + s_j/\Delta t)$$

$$c_{11} = e^{-\xi_j \omega_j \Delta t}[-(n_j - s_j/\Delta t)\cos(\omega_{dj}\Delta t) - (m_j - r_j/\Delta t)\sin(\omega_{dj}\Delta t)] - s_j/\Delta t \tag{35}$$

© 1998 John Wiley & Sons, Ltd.

$$c_{12} = -\mathrm{e}^{-\xi_j \omega_j \Delta t}\left[\frac{r_j}{\Delta t}\sin(\omega_{dj}\Delta t) + \frac{s_j}{\Delta t}\cos(\omega_{dj}\Delta t)\right] + (n_j + s_j/\Delta t)$$

$$c_{21} = \mathrm{e}^{-\xi_j \omega_j \Delta t}[-(n_j - s_j/\Delta t)\sin(\omega_{dj}\Delta t) + (m_j - r_j/\Delta t)\cos(\omega_{dj}\Delta t)] + r_j/\Delta t$$

$$c_{22} = \mathrm{e}^{-\xi_j \omega_j \Delta t}\left[\frac{r_j}{\Delta t}\cos(\omega_{dj}\Delta t) - \frac{s_j}{\Delta t}\sin(\omega_{dj}\Delta t)\right] - (m_j + r_j/\Delta t)$$

where

$$m_j + i \cdot n_j = \frac{G_j}{p_j}, \quad r_j + i \cdot s_j = \frac{G_j}{p_j^2} \tag{36}$$

REFERENCES

1. J. M. Kelly, *Theory and Practice of Seismic—Isolation Design*, Earthquake Engineering Research Center, University of California at Berkeley, 1996.
2. J. M. Kelly and E. Quiroz, 'Mechanical characteristics of neoprene isolation bearings', *Report No. UCB/EERC-92/11*, 1992.
3. F. G. Fan, G. Ahmadi, N. Mostaghel and I. G. Tadjabakhsh, 'Performance analysis of aseismic base isolation systems for a multistorey buildings', *Soil Dyn. Earthquake Engng.* **10**, 152–171 (1991).
4. F. G. Fan and G. Ahmadi, 'Floor response spectra for base-isolated multistorey structure', *Earthquake Engng. Struct. Dyn.* **19**, 377–388 (1990).
5. R. I. Skinner, W. H. Robinson and G. H. McVerry, '*An Introduction to Seismic Isolation*', Wiley, Chichester, 1993.
6. Uniform Building Code, *Earthquake Regulations for Seismic-Isolated Structures*, Vol. 2, Div. III, 1994.
7. N. M. Newmark, 'A method of computation for structural dynamics', *J. Engng. Mech. Div. ASCE* **85** (EM3) 67–94 (1959).
8. M. N. Hanna, 'An efficient mode superposition method for the numerical dynamic analysis of bilinear systems', *Ph.D. Dissertation*, University of California, Irvine, 1989.
9. P. Leger and S. Dussault, 'Non-linear seismic response analysis using vector superposition methods', *Earthquake Engng. Struct. Dyn.* **21**, 163–176 (1992).
10. B. Mohraz, F. E. Elghadamsi and Chi-Jen Chang, 'An incremental mode-superposition for non-linear dynamic analysis', *Earthquake Engng. Struct. Dyn.* **20**, 471–483 (1991).
11. R. Villaverde and M. M. Hanna, 'Efficient mode superposition algorithm for seismic analysis of non-linear structures', *Earthquake Engng. Struct. Dyn.* **21**, 849–858 (1992).
12. C. Pellegrino and F. Siano, *Analisi di Strutture Isolate Alla Base*, Cosmes, Napoli, 1993.
13. M. Ferraioli, P. Malangone, 'A modal superposition method for non-linear base-isolated multistorey structures', *XXV A.I.A.S Int. Conf.*, 1996, pp. 1161–1168.
14. 'Simqke: a program for artificial motion generation', Department of Civil Engineering Massachusetts Institute of Technology, 1976.
15. 'Eurocode 8, Earthquake resistant design of structures', (1993).
16. G. H. Powell, *Drain-2-D Program*, Earthquake Engineering Research Center, Berkeley, CA, 1973.
17. K. A. Foss, 'Coordinates which uncouple the equations of motion of damped linear dynamic systems', *J. Appl. Mech. ASME* **25**, (1958).
18. W. C. Hurty and M. F. Rubinstein, *Dynamic of Structures*, Prentice-Hall, Englewood Cliffs, NJ, (1964).
19. R. W. Trail-Nash, 'Modal methods in the dynamics of systems with non classical damping', *Earthquake Engng. Struct. Dyn.* **9**, 153–169 (1981).
20. C. J. Chang and B. Mohraz, 'Modal analysis of nonlinear system with classical and non-classical damping', *Comput. Struct.* **36**(6), 1067–1080 (1990).
21. A. J. Molnar, K. M. Vashi and C. W. Gay, 'Application of normal mode theory and pseudoforce methods to solve problems with nonlinearities', *J. Pressure Vessel Technol.* 151–156 (1976).
22. N. Mostaghel and J. Tanbakuchi, 'Response of sliding structures to earthquake support motion', *Earthquake Engng. Struct. Dyn.* **11**, 729–748 (1983).
23. N. C. Nigam and P. C. Jennings, *Digital Calculation of Response Spectra from Strong-motion Earthquake Records*, California Institute of Technology, EERL, Pasadena, CA, 1968.

© 1998 John Wiley & Sons, Ltd.